Comprehensive Experimental Study of a Starch/Polyesteramide Coextrusion

O. Martin, L. Avérous

Materials and Packaging Research Centre (ESIEC), BP 1029, 51686 Reims Cedex 2, France

Received 21 August 2001; accepted 4 February 2002

ABSTRACT: A comprehensive study of the three-layer film coextrusion was performed. Plasticized wheat starch (PWS) was chosen as the film central layer, and poly(ester amide) (PEA) was used as the surface outer layers. Single-screw extruders and a standard feedblock attached to a flat coat-hanger die were used to prepare the three-layer films. The layer deformation and interfacial instability phenomena, inherent to multilayer flows, were thoroughly investigated. The effect of process variables, such as viscosity ratio, extrusion rate, layer thickness, and die geometry, were studied. Encapsulation of the central layer by the skin layers readily occurred at the edges of coextruded films. The stability of PEA/PWS/PEA coextrusion flows was closely related to the shear stress at the interface. Increasing global volumetric flow rates and the die gap geometry seemed to promote instabilities. Finally, the existence of instabilities at the interface increased the adhesion strength of multilayered products, due to mechanical interlocking between adjacent layers. © 2002 Wiley Periodicals, Inc. J Appl Polym Sci 86: 2586–2600, 2002

Key words: rheology; adhesion

INTRODUCTION

The use of starch in nonfood applications has given rise to a large number of studies. As stated by Lörcks[1] in a recent article, starch may be a good alternative for the substitution of common petroleum-based polymers in specific applications, such as packaging. Native starch, once formulated with glycerol and water, can be transformed by traditional processing techniques, such as extrusion and injection molding. Processing and the properties of the resulting plasticized starch materials have been described in the literature.[2,3] Over the past decade, our laboratory has contributed significantly to the development of materials based on plasticized wheat starch (PWS), which is inline with the concept of sustainable development. For instance, we have studied the properties of PWS products, as a function of the processing conditions, the plasticizer content, and the storing conditions.[4] Materials ranging from stiff and brittle to soft and ductile were obtained, according to the plasticizer content. Thus, the properties of PWS products could be tuned, allowing fit with desired materials specifications. However, the high moisture sensitivity and rather low performance properties of PWS have constituted strong restrictions to the development of plasticized starch.

Combining plasticized starch with a hydrophobic polymer allows one to strengthen the properties of starch-based products. The choice of that polymer is made on prerequisites such as biodegradability, barrier properties, market availability, and cost. There may be different strategies used to improve plasticized starch properties, such as melt blending, extrusion coating, and coextrusion. As described in previous articles, melt blending PWS together with various biodegradable polymers, such as poly(ε-caprolactone),[5] poly(lactic acid)[6] (PLA), and poly(ester amide)[7] (PEA), has resulted in significant improvement of the physical properties of PWS and a marked decrease of the starch moisture sensitivity, even at low polyester concentrations (10 wt%). Among the various blends tested, a good level of compatibility was found between PWS and the aliphatic PEA. The association of PWS with PLA, although promising because both products are from renewable resources, did not yield satisfactory results in terms of compatibility. We showed that a thin polyester skin layer was formed at the surface of the blends during injection molding,[8] acting as a potential moisture barrier for starch. However, the starch moisture sensitivity was not fully addressed because of the blend phase distribution (the polyester was the minor component) and the low thickness of that outer skin. The case of extrusion coating, coating extruded films at the exit of die, has only been mentioned in the patent literature.[9] Its applicability with starch was questioned, and the molecular weight and process temperature of polyesters not appropriate for that process. Finally, the realistic development of moisture-resistant starch-based prod-

Correspondence to: L. Avérous (luc.averous@univ-reims.fr).
Contract grant sponsor: Europol' Agro.

ucts should be undertaken through multilayer coextrusion, which would allow one to prepare sandwich-type structures with PWS as the central layer and the hydrophobic component as the surface outer layers. Coextrusion seems the best option because it offers the advantages of a one-step, continuous, and versatile process.

Multilayer coextrusion has been widely used in the past decades to combine the properties of two or more polymers into a single multilayered structure.[10] However, some problems inherent to the multiphasic nature of the flow are likely to occur during coextrusion operations, such as nonuniform layer distribution, encapsulation, and interfacial instabilities, which are critical because they directly affect the quality and functionality of the multilayer products. There have been extensive experimental and theoretical investigations on these phenomena. The layer encapsulation phenomena corresponds to the surrounding of the more viscous polymer by the less viscous one, as shown by Lee and White.[11] Experimental investigations on the shape of the interface were reported by Southern and Ballman,[12] and Khan and Han,[13] who showed that viscosity differentials between respective layers dominates over elasticity ratios. Inversely, White et al.[14] reported the influence of normal stress differences on the shape of the interface. In recent experimental studies, Dooley and colleagues[15,16] investigated layer rearrangement during coextrusion and the importance of the flow-channel geometry. They indicated that coextrusion of identical polymers, that is, with matched viscosities, can lead to layer rearrangement, due to the die geometry.

Yih[17] and Hickox[18] pioneered studies on interfacial instabilities, suggesting that viscosity differences may cause instabilities of stratified flow. Schrenk and Alfrey[10,19] investigated the factors responsible for the onset of instabilities and suggested the existence of a critical shear stress value beyond which interfacial instabilities are likely to occur. Han and Shetty[20,21] described in detail the factors responsible for the occurrence of instabilities, such as critical shear stress at the interface, the viscosity and elasticity ratios, and the layer thickness ratios. In addition, many authors[22–30] have modeled multilayer flows through computer simulation and attempted to elucidate the influence of viscoelasticity, layer thickness, and die geometry on layer rearrangements and the onset of instabilities. Karagiannis et al.[22] modeled the encapsulation phenomenon, and Sornberger et al.[23] studied the interface position in a two-layer flat film coextrusion. In a recent work, Gifford[24] attempted to account for viscoelasticity effects on layer deformation. However, to date, most numerical investigations have only partly addressed the layer uniformity problem due to the complexity of the stratified flow systems. Khomami and coworkers[25–29] contributed significantly to the understanding of the onset and propagation of interfacial instabilities and of interface deformations, thanks to a specially designed optical interface monitoring system that allows one to visualize, after image reconstruction, the multilayer flow in the die. Khomami[25] and Su and Khomami[26,27] examined the elastic and viscosity effects on the interfacial stability, according to the die geometry and layer depth ratio. They determined the role of elasticity in the mechanism of instabilities. Wilson and Komani[28,29] studied experimentally and numerically the propagation of periodic flow disturbances and determined the stable and unstable flow conditions, finding a good agreement with models. In a recent study, Tzoganakis and Perdikoulias[30] studied experimentally the effects of material properties and flow geometry on the appearance of interfacial instability. Surprisingly, despite the number and diversity of studies on multilayer flows and stability, only a few have reported on the use of plasticized starch and polyester in the coextrusion processes,[31] although they are of indubitable interest as innovative materials. Moreover, no detailed study is available to date in the literature that has addressed the influence of the process variables on flow stability.

The aim of the study was to correlate the layer deformation and the appearance of interfacial instabilities on polyester/PWS/polyester films with the flow conditions, viscosity ratio, and layer thickness ratio. The influence of the flow geometry was also investigated. PEA was chosen as the outer-layer component because it is readily biodegradable, moisture resistant, and rather compatible with PWS without the use of specific compatibilizers. In our first approach, low-density polyethylene (LDPE) was used as a model. The conditions for the stability of multilayer flows are reported, and the effect of instabilities on the adhesion

TABLE I
Compositions of the Various PWS Types

PWS type	Starch content[a]	Glycerol content[a]	Glycerol/starch ratio[a]	Moisture content[a]	Density
PWS1	74 (80)	10 (11)	0.14 (0.14)	16 (8.5)	1.39
PWS2	70 (73)	18 (18)	0.26 (0.25)	12 (8.7)	1.37
PWS3	65 (57)	35 (30)	0.54 (0.52)	0 (12.6)	1.34

[a] Compositions of the Pw-PWS blends are given in weight percentage of total wet basis, and values between parentheses were determined on Pe-PWS pellets after equilibration at 23°C and 50% RH.

TABLE II
Physical Characteristics of the Polymers

Material	Density	*Ko** (Pa.s^m)	*E/R* (K)	Young's modulus (MPa)	Tensile strength (MPa)
PWS1	1.39	19300	4500	982	17.4
PWS2	1.37	12600	5860	89	3.4
PWS3	1.34	10350	5860	31	2.1
PEA	1.26	9920	3360	260	19
LDPE	0.92	9000	1960	220	12

strength of resulting biodegradable multilayer films is shown.

EXPERIMENTAL

Materials

Native wheat starch was purchased from Chamtor (Pomacle, France). The starch contained 74% amylopectin (the branched component) and 26% amylose (a linear carbohydrate polymer). According to the supplier, the residual protein and lipids content were less than 0.2 and 0.7%, respectively. Glycerol with 99.5% purity was used as a plasticizer. Various PWS samples (PWS1, PWS2, and PWS3), differing in the glycerol to starch ratio, were prepared. The procedure used to prepare PWS from native starch was detailed in a previous article.[6] Table I shows the different PWS formulations prepared. Both powdery plasticized wheat starch (Pw-PWS) and extruded plasticized wheat starch (Pe-PWS) products were used in the study. The aliphatic PEA was kindly supplied by Bayer (Walsrode, Germany). We used an extrusion-grade PEA, designated by the name LP BAK® 404. The LDPE used was Lacqtene 1070MG24 grade, obtained from AtoFina (Harfleur, France). Table II presents the physical characteristics and rheological parameters of all the materials used in this work.

Processing and procedures

The experimental setup for the coextrusion of multilayer films consisted of two single-screw extruders, a feedblock attached to a wide flat die, and a three-roll (diameter = 150 mm) calendering system. A specially designed torpedo screw was used for the extrusion of starch, and a 30 mm diameter, 26:1 length to diameter ratio (L/D) single screw extruder was used for the cap layer. Figure 1 presents a schematic view of the flat coat-hanger die with the feedblock attachment. The die was constituted by a rectangular entry channel (50

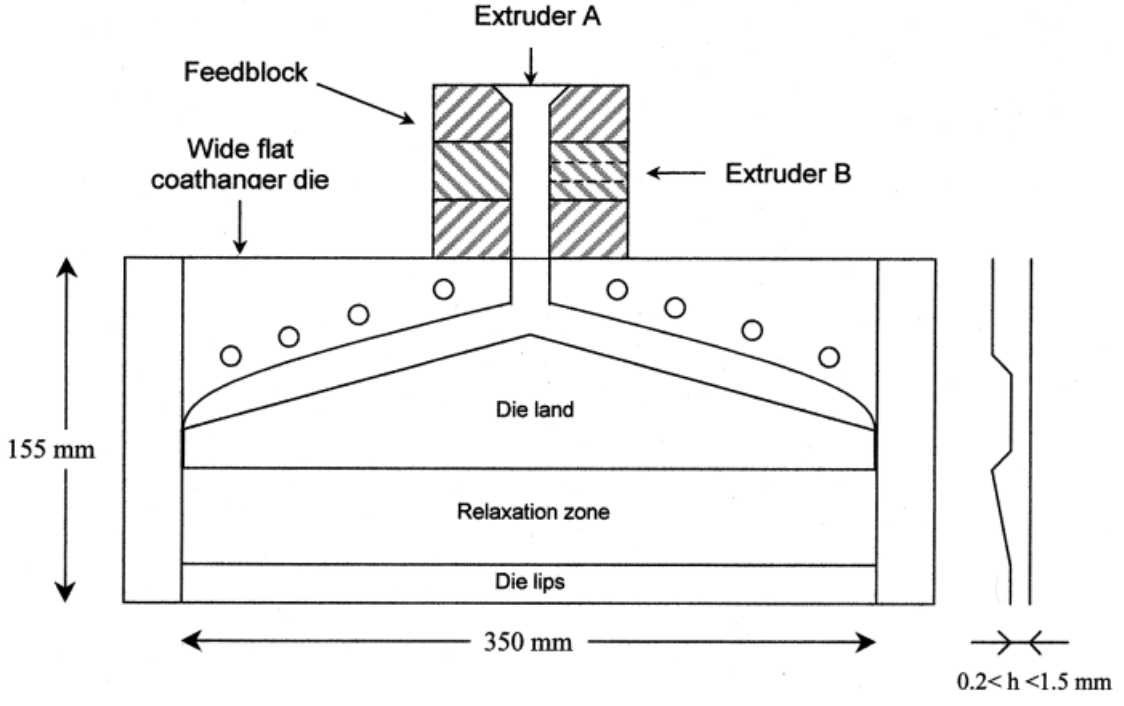

Figure 1 Schematic view of the feedblock and flat coat-hanger die (the feedblock consisted of three modules put together; the first one was the manifold module, the medium one was the feedport module, and the last one was the transition module).

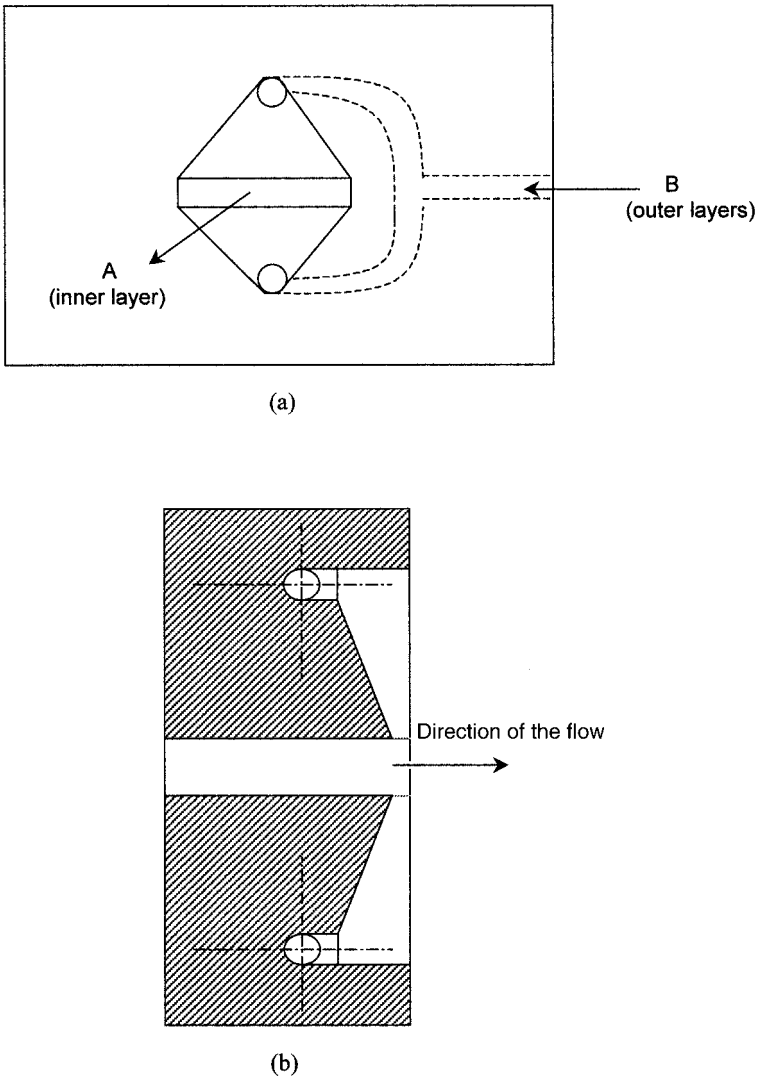

Figure 2 (a) Front view and (b) transverse cross-section of the medium block of the feedblock. The rectangular flow channel of the feedblock was 30 × 120 × 4 mm, and the side stream inlet tube diameter was ϕ = 8 mm.

× 30 × 4, mm), a coat hanger of decreasing cross section, a die land area of adjustable height, a relaxation area of decreasing thickness (from 4.5 to 1 mm), and finally, the die lips (length = 350 mm). The schematic of the feedblock, which allowed the polymer melt from each extruder to be combined into a stratified three-layer melt stream, is shown in Figure 2. The feedblock was designed to receive two feed streams, and the slit section had the following dimensions: length = 120 mm, width = 30 mm, and thickness = 4 mm. As shown in Figure 1, the three blocks were put together to form the feedblock. The melt stream forming the outer layers (extruder B in Fig. 1) was split by half along two flow paths [Fig. 2(a)] and then merged with the main polymer stream (inner layer, from extruder A) in the slit section 30 mm before the flat die entry. From the die inlet, the melt streams could flow through the die inlet and spread uniformly across the entire width of die. The spreading of the three-layer flow across the die was due to the coat-hanger geometry, that is, the restriction of the channel section along the flow direction. The die land area (see Fig. 1), which section was determined by a restriction bar, was adjustable in height by a change to the thickness of the moveable restriction bar. The die land channel height could be varied from 1.5 to 3.5 mm. Consequently, the flow path profile along the axial direction could be modulated from distorted to relatively smooth.

In routine experiments, the coextrusion line was run for at least 30 min to ensure steady state operations. Initially, the flow rates of all polymers used were measured independently for each extruder at the corresponding screw speeds so that the A:B flow ratio could be controlled. In all experiments, the outer layer was always the minor component. After exiting the die, the coextruded film was cooled with the chill roll and collected to analyze the magnitude and periodicity of the wavy instabilities. A cooling air jet was

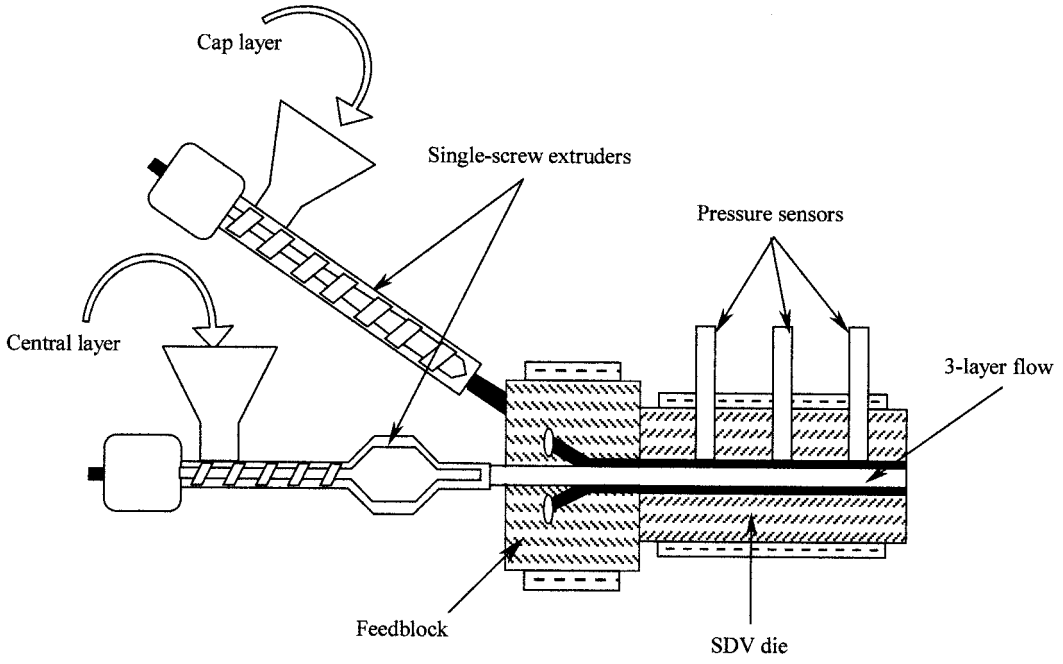

Figure 3 Schematic illustration of the feedblock–SDV assembly system to determine the rheological properties of monolayer and multilayer flows.

applied in some cases on the film exiting the die, especially when the higher moisture content PWS was used, to prevent water vapor bubble growth. The plasticized starches were processed in a temperature range between 110 and 150°C, and the outer layer polyester (PEA) was processed at 150, 175, and 200°C. Excessive melt-temperature differentials between respective layers had to be avoided.[10] The temperature of the film-forming die was set close to 150°C in all experiments. In most cases, when the steady state conditions were reached, the multilayer film was collected, and then extruders were stopped simultaneously, and the die rapidly cooled to room temperature. Once solidified, the polymer sprue was removed from the die and cut into pieces. This procedure allowed us to measure the position of the interface at each point of the die. In some cases, the flow characteristics of combined melt streams were measured with the feedblock–slit die viscometer (SDV) assembly, as illustrated in Figure 3. The SDV consisted of an instrumented slit section, of which principles and data treatment were described in a previous article.[32] This procedure allowed us to measure the flow properties (axial pressure gradient, and shear stress at wall) of the combined flow streams at the exit of the feedblock.

Characterization

Melt rheology

The viscosity of all products used in coextrusion experiments was measured thanks to a specially designed SDV. The use of this system was described in a previous article.[32] The reader is invited to refer to that article for details. Each product was tested at temperatures close within ± 4°C of the melt temperature in the flat die. Shear rates in the range of 1–1000 s^{-1} were obtained. The PWS products (Table 1) were tested in both powdery and pellet forms.

Peel testing

Peel tests were carried out on a Twin-Albert peel tester (model 225-100) at a rate of 50 mm/min. The test specimens were cut from the coextruded film into 100 × 20 mm strips. The outer polyester layer was delaminated mechanically and gripped onto the load cell, and the film was secured on a sliding plate so that a constant 90° angle between the polyester layer and PWS was maintained during the test. Load-data collection started after 3 s of prepeel. A mean value was determined from each test, and each sample was tested five times.

Optical microscopy

A Leitz microscope was used to capture the shape of the interface between the respective layers of coextruded structures. Both tinted LDPE three-layer films and PEA/PWS/PEA films were examined. Each films were either freeze fractured or cut with a diamond-like precision saw. We stained the PWS phase with iodine vapor obtained from resublimed iodine crystals to better differentiate layers. The amplitude of wave-

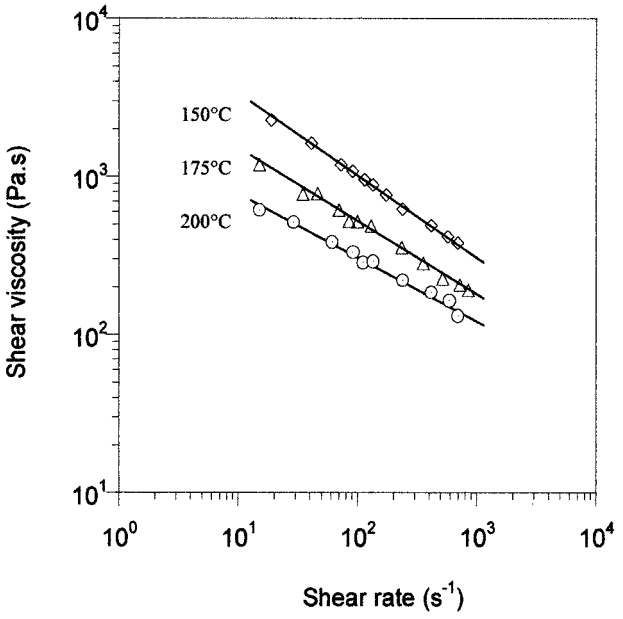

(a)

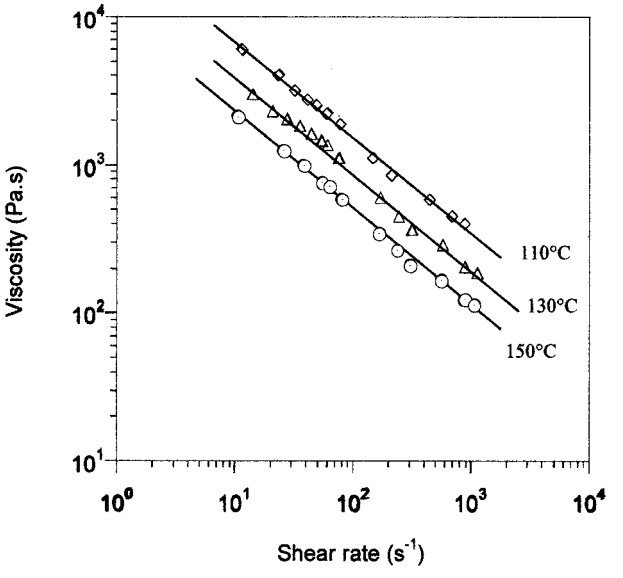

(b)

Figure 4 Rheological properties of (a) PEA and (b) PWS at various temperatures.

like instabilities at the interface were measured with Leitz image-analysis software.

RESULTS AND DISCUSSION

The rheological properties of PEA and PWS products are presented in Figure 4. The viscosity values of all PWS products determined with the slit die rheometer were presented in detail in a previous article.[32] For instance, the melt viscosity of PEA lay around that of molten PWS, depending on the temperature and shear-rate range. Melt viscosity ratios between PWS and PEA ranging from 1 to 5 could thus be obtained, thanks to the controlled process temperatures of the respective polymers. It should be noted that melt temperatures of PEA below 150°C could not be obtained because fluctuations in the extruder torque would occur below that temperature. The latter comment is important because unsteady torque at given screw speed is known to cause flow disturbances due to pressure variations, which are likely to promote interfacial instabilities, as described by Khomami and colleagues.[25–28] Due to the complexity of multilayer flows, our attention first focuses on the effect of operating conditions and viscosity ratios on the layer uniformity and then on the mechanisms giving rise to instabilities at the interface.

Interface deformation

A series of experiments was carried out with the extruders and feedblock only (without any die attached to it) to check whether the three layers were evenly distributed and were uniform in thickness at the exit of the feedblock. Extrusion-grade LDPE was used in both extruders in these trials. To better distinguish the interface between respective layers, we pigmented the central layer black and pigmented the cap layers

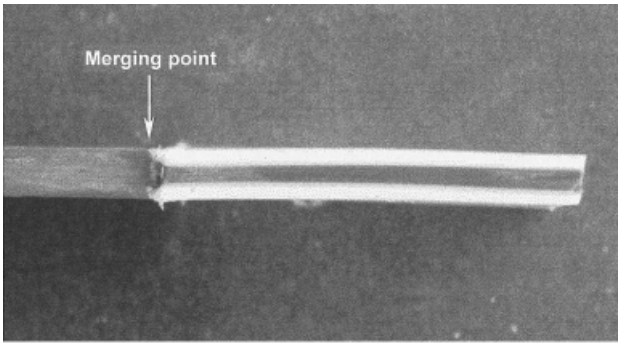

(a)

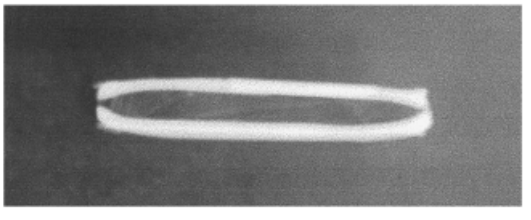

(b)

Figure 5 Cross-section of the three-layer coextruded polyethylene in the feedblock. The temperature conditions were (a) T = 130°C for both layers, and (b) T = 130°C for the inner layer and T = 150°C for the outer layers.

white. Figure 5 shows photographs of the transverse section of the three-layer solidified sprue, reflecting the real flow conditions in the feedblock, that is, upstream of the die entry channel. Uniform layer distribution and flat interfaces were obtained when the LDPE melt streams had similar melt temperatures. However, when a melt differential as low as 30°C was imposed, the outer layers started to surround the central layer along the 30-mm flow length (from the merging point to the feedblock exit). That configuration, consisting of a higher melt temperature and a lower viscosity polymer as the cap layers, was chosen to reflect the conditions of the PWS and aliphatic polyester coextrusion. The temperature processing range of PWS was limited due to starch degradation, and plasticized starch melt viscosity was generally higher than that of PEA. The layer rearrangement, where the less viscous outer layers start to surround the other layer, is called *encapsulation*. The encapsulation of the more viscous layer by the less viscous one is a well-known phenomenon and has been extensively dealt with in the literature. For instance, Lee and White[11] and Southern and Ballman[12] showed that when the viscosity ratio increases, the degree of encapsulation increases accordingly. The interface shape change seen in Figure 5 was explained by the principle of viscous encapsulation. Layers rearrange themselves to minimize the total energy. The encapsulation effects could thus be limited by a reduction in the viscosity difference of the respective layers.

The viscosity difference between respective layers is not the only factor inducing encapsulation. The shape and length of the flow channel also have a nonnegligible influence over that phenomenon. When the three-layer system with a viscosity ratio close to unity was processed through the feedblock and SDV assembly (see Fig. 3), some degree of encapsulation was found at the exit of the SDV die. The explanation lies in the fact that the cap layers in contact with the die wall were exposed to higher shear stresses and greater heat dissipation than the central layer, resulting in a progressive change in the viscosity. A specific geometric design of the flow channel may compensate for these effects. Some authors[33] have described die designs that allow one obtain flat interfaces at the exit of feedblocks for instance. However, in our case, the geometry of the wide film die used in the coextrusion experiments was only adjustable at the die lips, and the encapsulation started even before the die entry channel. When PWS and PEA were coextruded together, the PEA cap layers almost encapsulated the central layer, regardless the flow conditions. The cap component commonly encapsulated the central layer at the side wall of the die. The *degree of encapsulation,* referring to the percentage area surrounded by the outer layers, ranged from partial (0–50%) to total (100%) in the film-forming die. Decreasing the cap layer flow-rate usually resulted in a decrease of the extent of encapsulation on the edges of film, from 10–15 mm down to 2–4 mm. However, the occurrence of encapsulation was not thought to be very critical in our case because it commonly affects the edges of the coextruded structures only, which are usually discarded.

Interfacial instability

Unlike encapsulation effects, the occurrence of interfacial instabilities was very critical because it directly affected the quality and functionality of the coextruded films. Figure 6(a) is an illustration of the velocity profile of a three-layer flow through a slit die of gap $y = h$. Because of the symmetry, only one half of the channel height was considered. Under stable flow conditions, the interfaces of the final multilayer film may have been flat and smooth. Inversely, interfacial instabilities manifested themselves as wave-like distortions of the interface between the two polymers across the width of the film, as shown by the schematic of Figure 6(b).

In the system studied, which consisted of shear-thinning polymers in simple shear flow, several mechanisms could give rise to interfacial instabilities. According to our experimental results, interfacial instability set in within the die. The variables known to play an important role in the occurrence of instabilities are the skin-layer viscosity, the layer thickness ratio, the total extrusion rate, and the die gap. Moreover, interfacial instabilities are known to result when a certain shear stress value at the interface of two polymers is exceeded. The onset of interfacial instabilities can thus be characterized by the critical interfacial shear stress (CISS). The interfacial shear stress τ_{int} can be calculated from the known coextrusion conditions and the flow characteristics by the equation:

$$\tau_{\text{int}} = \tau_w y_{\text{int}}/(h/2) \tag{1}$$

where τ_w is the shear stress at the die wall (at y = h/2), y_{int} is the position of the interface, and h is the slit height (see Fig. 6). The shear stress at wall is determined by the expression:

$$\tau_w = (-\partial p/\partial z)\frac{h}{2} \tag{2}$$

where $(-dp/dz)$ is the axial pressure gradient measured by the wall normal stress measurement.

As indicated by eq. (1), determining the position of the interface for a given flow ratio is important. To measure the interface positions inside the die, we cut

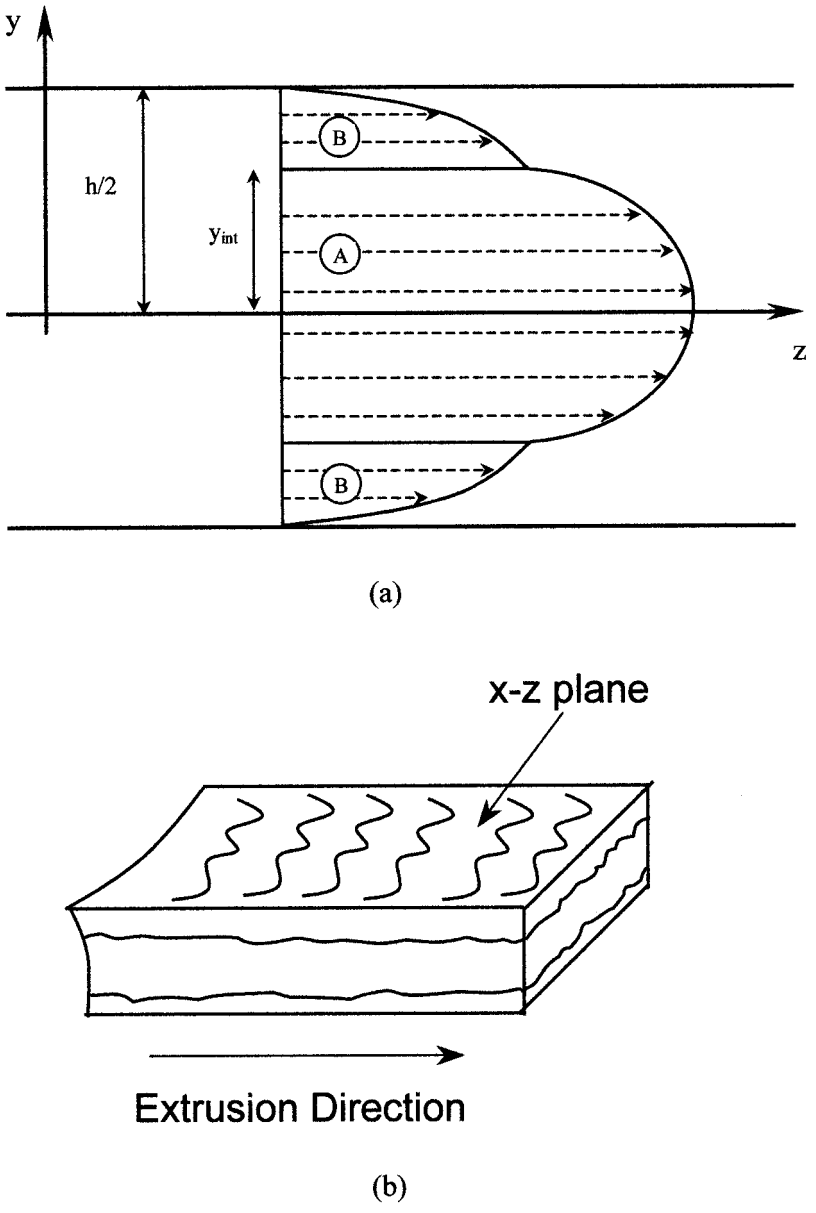

Figure 6 (a) Velocity profile of a three-layer flow through parallel plates and (b) schematic of the multilayer film exhibiting wavy instabilities at the interface.

the solidified sprues obtained from different experiments into slices along the flow direction, as presented in Figure 7. In the absence of a direct visualization inside the flow channel, the cross-sections [Fig. 7(b)] of the sprue allowed us to determine the repartition of layers in the distribution channel, the flow restriction zone, the relaxation zone, and the die lips, respectively. The exact position of interface was measured with binoculars.[34] Note that from the center to the edge of the die (cross-sections A-A and C-C, respectively), the outer white layer encapsulated the central layer, could be seen from the decreasing black layer thickness from the center to the edge. The influence of each variable was investigated, whereas other conditions were kept constant, and the flow conditions from stable to unstable were obtained. At the point of incipient instabilities, the CISS could be calculated with the known flow conditions and eqs. (1) and (2).

Effect of the viscosity ratio and the layer thickness ratio

In a first approach, we ran the same LDPE three-layer system mentioned previously through the feedblock and SDV assembly to obtain stable and unstable flow conditions and to determine the effect of viscosity and the layer thickness ratio. We varied the flow ratio was varied to obtain the layer thickness ratios h_B/h_A (the subscript A denotes the central layer, and B denotes the cap layer) ranging from 0.2 to 2; the total volumet-

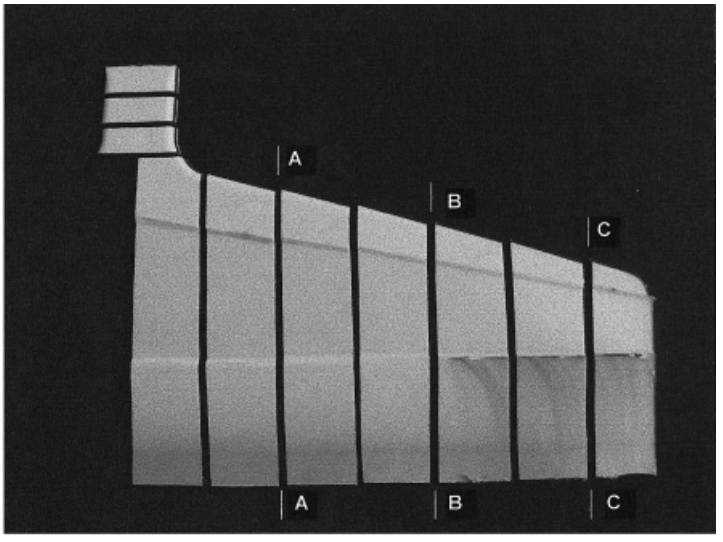

(a)

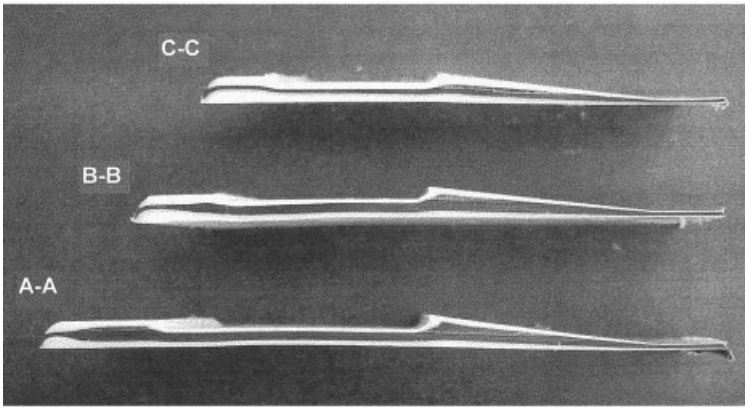

(b)

Figure 7 Photographs of the (a) sprue cuts on one half of the flat die and (b) interface positions along the cross-sections.

ric flow rate ($Q = Q_A + Q_B$) was also increased from 50 to 160 g/min. In the same manner, LDPE melts of differing viscosity were coextruded together through the SDV die. Figure 8 presents the shear stress at the wall as a function of the layer thickness ratio for the three-layer LDPE system at various viscosity ratios (ratios of 0.5, 1, and 2 were set). Although the limit between the stable and unstable interface was not obvious, high shear stresses resulting from high extrusion rates gave rise to interfacial instabilities. That trend was even more clear when the cap layer was the higher viscosity component. Inversely, when the cap component was the low-viscosity layer (triangular symbols), the instabilities could set in at a high extrusion rate only (i.e., high total volumetric flow rate) or low layer thickness ratio. This could be explained by the fact that when the less viscous component surrounded the more viscous layer, the wall pressure gradient of the combined melt streams decreased significantly, even below that of constitutive polymers, thus reducing the shear stress level at the wall. This observation is consistent with Han and Shetty's[20,21] findings on LDPE/polystyrene and LDPE/high-density polyethylene three-layer systems. The coextrusion experiments on the three-layer LDPE system reflected the flow behavior of the combined melt streams and showed that viscous stratification or a thin outer layer could cause instability. However, this system was simply used as a model because it could not take into account the specificity of the PWS and PEA system, notably in terms of viscoelastic behavior and compatibility.

The Pw-PWS and PEA were coextruded together through the feedblock and the wide flat film die. The conditions for the coextrusion of the PEA/PWS3/PEA three-layer system are reported in Table III. Only the total flow rate (Q_T) was measured, and the individual flow rates were derived from the total flow rate and those determined from corresponding extruder speeds. We maintained the total flow-rate in the same

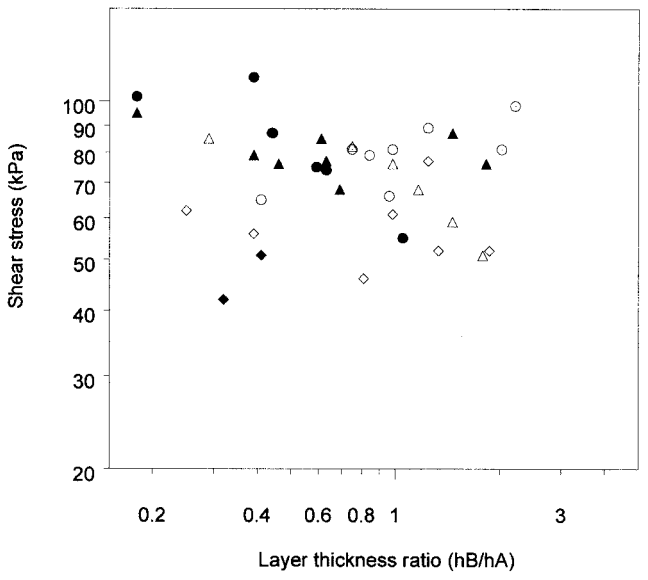

Figure 8 Plot of the wall shear stress versus the layer thickness ratio for different viscosity ratios of the three-layer LDPE system: (○, ●) $\eta B = \eta A$, (△, ▲) $\eta B/\eta A = 2$, and (◇, ◆), $\eta B/\eta A = 0.5$. Filled shapes denote unstable flow regions, whereas white ones represent stable flow conditions.

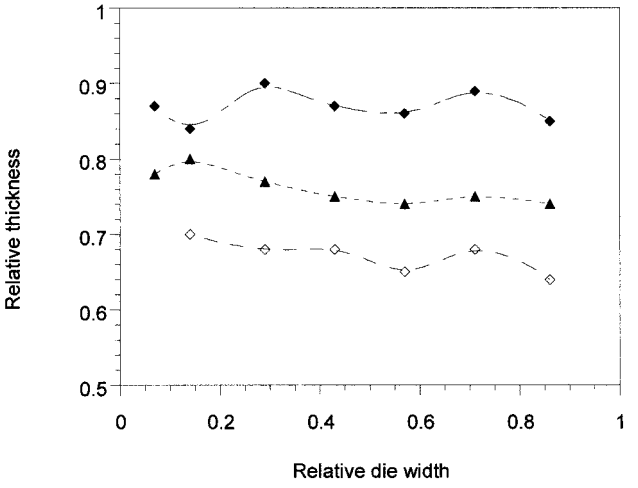

Figure 9 Interface positions across the wide die exit of PWS3/PEA/PWS3 films at 150°C. From top to bottom, the flow ratio Q_{PEA}/Q_{PWS} is 0.26, 0.36, and 0.64.

range in all experiments to study the effects of viscosity and thickness ratio only. The flat die temperature was set close to the higher melt temperature layer so that the combined stream did not solidify at the die wall. The interface positions across the entire width of film at the die exit corresponding to experiments 5, 6, and 7 in Table III are shown in Figure 9. The interface was not flat due to some irregular layer distribution. At both edges of film, no interface could be measured because the PEA layer surrounded the PWS layer. The encapsulation that began in the feedblock was enhanced by the flow through the die because about 10–15 mm of each edge of film was encapsulated by the cap layers. The coextrusion of the PWS/PEA three-layer system through the wide film die mostly led to unstable flow conditions, even when the viscosity of respective layers were matched (experiments 5–8) and whatever the layer thickness ratio. Note that these experiments were performed with the narrow die gap geometry, that is, a channel height in the die land area as low as 1.5 mm.

Because changing variables such as the viscosity of products and the layer thickness ratio did not yield satisfactory results, the flow behavior of the combined streams were investigated with the instrumented SDV flow channel. Flow conditions similar to those in Table III were used, exept that the overall flow rate was varied from 60 to 180 g/min. We assumed that the locations of interfaces inside the SDV die were equivalent to those at the wide flat die entry channel measured from the solidified sprue (Fig. 7). As stated previously, the pressure gradient and interface posi-

TABLE III
Experimental Coextrusion Conditions of the PEA/PWS3/PEA Three-Layer System

Experiment	Q_T (g/min)	h_{PEA}/h_{PWS}	Melt temperature T_{PWS} (°C)	Melt temperature T_{PEA} (°C)	τ_{int} (kPa)	Stability
1	88.0	0.24	110	150	65	Unstable
2	86.4	0.38	110	150	52	Small instabilities
3	98.2	0.58	110	150	51	Stable
4	90.4	0.79	110	150	42	Stable
5	81.9	0.26	130	150	86	Unstable
6	87.0	0.36	130	150	90	Unstable
7	91.5	0.64	130	150	48	Minor instabilities
8	95.9	0.84	130	150	56	Unstable
9	87.3	0.27	150	150	73	Unstable
10	90.2	0.35	150	150	64	Unstable
11	94.4	0.55	150	150	55	Stable
12	92.8	0.81	150	150	68	Unstable

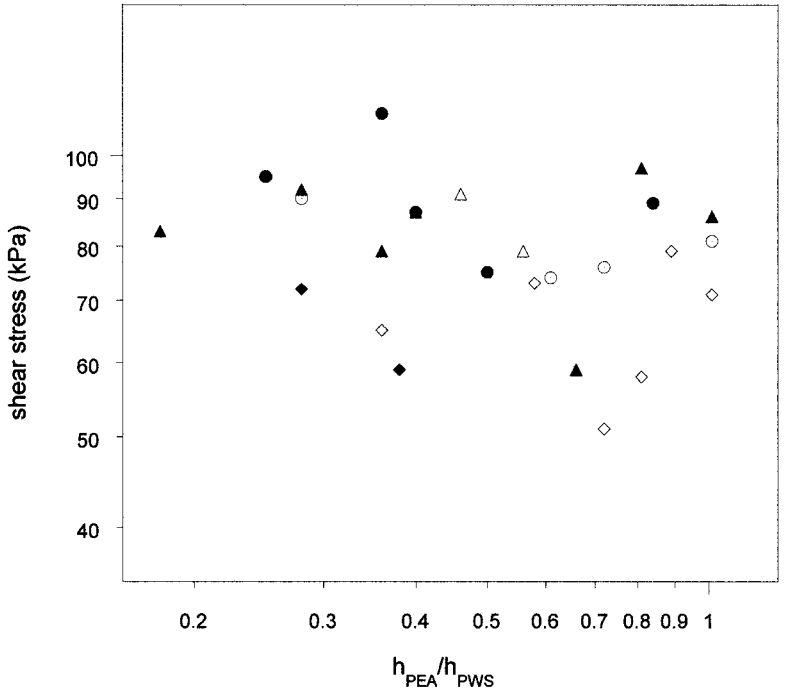

Figure 10 Plot of the wall shear stress versus the layer thickness ratio of PEA/PWS/PEA coextruded films: (○, ●) $\eta B/\eta A = 1$, (△, ▲) $\eta B/\eta A = 4$, and (◇, ◆) $\eta B/\eta A = 0.3$. Filled shapes denote unstable flow regions, whereas white ones represent stable flow conditions.

tions allowed us to calculate the wall shear stress and the interfacial shear stress. Figure 10 shows the plot of the shear stress as a function of the layer thickness ratio. Despite the scattering of data points, there seemed to exist a physical limit between the stable and unstable regions. As shown in Figure 10, when the cap layer was the low-viscosity component, with a layer ratio between 0.5 and 1 and at moderate wall shear stress, some extent of flow stability could be obtained. This result, similar to that found in the case of the LDPE system, seemed to indicate that the lower viscosity cap layer had a stabilizing effect on the multilayer flow. Inversely, low layer thickness ratios or high shear stresses readily induced instabilities, whatever the viscosity ratio. From these results and the known interface position inside the die, the corresponding values of interfacial shear stress were computed. It seemed that higher shear stresses at the interface, due to higher flow rates or lower cap layer thickness, were responsible for the onset of instabilities in the multilayer flow. There seemed to be a range of CISS above which interfacial instabilities set in, depending on the layer thickness ratio. However, previous studies[21,22,35] on three-layer films showed that there existed a single CISS value for a given polymer system, which is independent on the varied process parameters, including layer thickness ratio. For our three-layer system, no such value of CISS was found, because values at incipient instabilities ranged from 52 to 64 kPa and because instability-free flows were observed beyond 55 kPa. These results are in apparent contradiction with previously published ones, probably due to the complexity of the system studied and specificity of PWS rheological behavior. It may be concluded from this section that the low layer thickness ratio and viscosity differences with the cap layer as the more viscous component are likely to promote instabilities.

Effect of the extrusion rate and die geometry

The *extrusion rate* refers to the magnitude of the total volumetric flow rate measured at the exit of the die. Enhancing extrusion rates results in increasing pressure gradients and, thus, increasing shear stresses at the die wall. As shown by Han and Shetty[20] in a study on film coextrusion, the shear stress is continuous across the interface. Therefore, higher interfacial shear stresses may be reached at high extrusion rates. Moreover, as indicated earlier, the height of the slit section of the die land may be varied between 1.5 and 3.5 mm. As a result, an increase in the height of slit section upstream of the relaxation zone is expected to cause a reduction of the global pressure drop across the die, thus reducing the shear stress level.

The next experiments were aimed at reducing the shear stress in die. We varied the flow rates of individual melt streams accordingly to increase the extrusion rate across the flat film die of decreasing slit height. The resulting total flow rate was measured at

TABLE IV
Effect of the Extrusion Rate and Die Geometry on the Stability of Coextrusion flows

Experiment	Die temperature (°C)	Q_T (g/min)	Global pressure drop[a]			Flow stability[b]		
			G_1 (MPa)	G_2 (MPa)	G_3 (MPa)	1	2	3
1	150	48	4.6	3.1	2.5	s	s	s, bld
2	150	56	5.1	3.9	3.1	u	s	s, bld
3	150	65	5.8	5.2	4.0	u	s, bld	s, bld
4	150	78	6.8	5.8	4.5	u	s, bld	u, bld
5	150	91	7.8	6.4	4.9	u	u, bld	u, bld
6	150	112	8.6	7.1	5.5	u	u, bld	u, bld

[a] The subscripts 1, 2, and 3 designate the height of slit section in die land area of 1.5, 2.5, and 3.5 mm, respectively.
[b] *s* designates a stable flow, *u* designates an unstable flow, and *bld* means bad layer distribution.

the die exit, and the global pressure drop was recorded. The corresponding data are shown in Table IV. The most striking result was that nearly no flow stability could be obtained with the narrow die gap geometry (G1 with $h = 1.5$ mm), whereas some instability-free three-layer films were obtained through the larger die land slit section. Increasing the die temperature to 170°C did not seem to help. For a given extrusion rate, increasing the die land slit section induced a significant decrease in the shear stress at the wall and at the interface. For instance, in experiment 5, the shear stress ranged from 105 to 44 kPa between the G_1 and the G_3 geometries. However, poor layer distribution resulted from the increase in the slit height. The reduction of interfacial instabilities was achieved at the expense of the uniformity of the product. The magnitude of shear stress change due to geometry modulation and extrusion rate variation was significant. Increasing extrusion rates and reducing the flow section both favored the onset of instabilities. These results are in good agreement with previously published ones. We conclude that the film coextrusion of polymers is a compromise between many factors and that the influence of each parameters need to be fully ascertained.

Effect on the strength of interface

As detailed in a previous study[36] the adhesion strength between the layers of a coextruded structure rely on the compatibility of respective materials only when no tie layer is used. Because the occurrence of interfacial instabilities is a recurrent problem in the field of coextrusion, it may also alter the final adhesion between layers. Ranjbaran and Khomami[37] showed that a controlled amount of instabilities can significantly increase the interfacial strength of multilayers, because of mechanical interlocking. They presented photographs of compatible and incompatible polymer pairs with varying extents of mechanical interlocking. Wang et al.[31] also described the possible advantages of instabilities in terms of interfacial bonding increases.

We saw that the occurrence of interfacial instabilities is closely related to the shear stress at the interface. As a result, there may be several ways to increase the instabilities in a coextruded film, such as increasing the extrusion rate, lowering the thickness of cap layers, or reducing the gap in the die land area. Moreover, adjusting the viscosity of cap layers above that of PWS is likely to favor instabilities. In Table V, varying conditions were selected to generate stable and unstable coextrusion flows. In experiments 1 and 2, no instabilities were obtained, leading to moderate interfacial strength values. In experiments 3-6, the extrusion rate was increased, and the skin layer thickness was reduced, thus giving rise to marked instabilities in PWS/PEA films. In that case, the peel strength increased up to 70% compared to instability-free multilayers. The standard deviations (experiments 5 and 6) greatly increased because strong fluctuations were

TABLE V
Effect of Instabilities on the Interfacial Strength of Multilayer PEA/PWS3 Films

Experiment	Film thickness (μm)	h_{PEA} (μm)	Pressure drop (bar)	Interfacial instabilities:[a] mean wave amplitude (μm)	Peel strength[b] (N/mm)
1	920	180	50	None	0.15 (0.03)
2	870	120	58	None	0.16 (0.03)
3	880	105	70	70	0.19 (0.02)
4	890	90	68	80	0.20 (0.02)
5	910	100	82	90	0.24 (0.08)
6	850	95	78	140	0.26 (0.08)

[a] The amplitude of wave-like instabilities was measured with the calibrated image-analysis software.
[b] Standard deviations are given between parentheses.

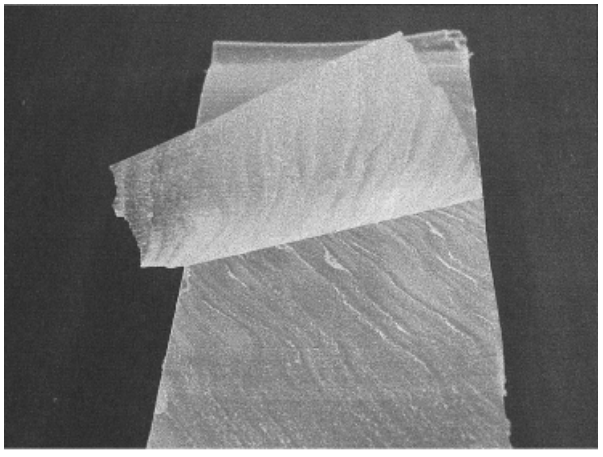

(a)

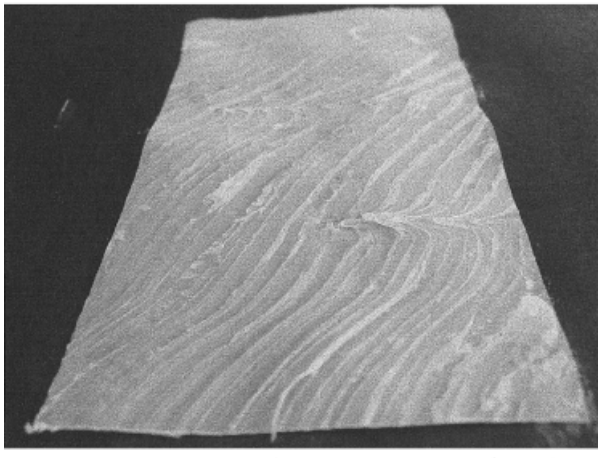

(b)

Figure 11 Photographs of films exhibiting wave-like instabilities of different amplitudes and frequencies: (a) small amplitude waves visible on the PWS layer and the PLA peeled layer and (b) severe instabilities on the PEA peeled layer.

found in the adhesion during the tests due to wavy instabilities. Photographs of the mechanically peeled surface showing different degree of instability are presented in Figure 11. As shown in Figure 11(a), the low-amplitude wave instabilities may have limited the ties between layers. Note that Figure 11(a) also gives a clear illustration of the encapsulation on the edge of the film. Inversely, significant mechanical interlocking may have been obtained in the case shown in Figure 11(b) due to the frequency and amplitude of striations. Figure 12(b,c) shows microscopic images of the cross-sections of PWS/PEA sprues, giving evidence of the penetration of the PEA layer in the PWS phase. These observations were made on the relaxation zone of the die. Figure 12(a) clearly shows that the amplitude of wave-like instabilities was dependent on the shear rate. The amplitude of instabilities could be varied by a gradual increase in the shear stress. In Figure 12(b,c), the dark phase is the PWS (stained with iodine vapor), and the yellowish outer phase is the PEA. The amplitude increased from 50 to 170 μm [as shown in Fig. 12(c)] as the shear stress increased. However, that clear trend was not observed in all of the coextrusion experiments. For instance, high-amplitude instabilities, resulting in strong bonding between layers, were found for the PEA/PWS1/PEA system under conditions similar to those of experiments 1 and 2 (Table). Certain mechanisms giving rise to instabilities could not be controlled, such as elasticity differences between layers, die exit phenomena, or velocity profile differences.

CONCLUSIONS

The layer uniformity and interfacial instability phenomena in the three-layer coextrusion of the PEA/PWS/PEA system were thouroughly studied. Experimental results showed that the skin-layer viscosity and thickness, the global extrusion rate, and the die geometry were key parameters, which is in agreement with previous findings. We found that reasonable layer uniformity could be obtained across the width of the die and that encapsulation of the central starch layer could not be avoided, even when the cap layers were the high-viscosity component. However, sidewall encapsulation was not thought to be very critical. Close attention was given to the interfacial instabilities because they may have been more detrimental to the coextruded product. The occurrence of instabilities was strongly related to the shear stress at the interface. Flow conditions ranging from stable to unstable were obtained. CISS values from 48 to 64 kPa were calculated from the flow equations and the known experimental conditions. Investigations of the flow behavior of plasticized starch/PEA multilayers allowed us to classify the onset of instabilities according to the dominating factors. Viscosity differences, high extrusion rates, and low cap layer thicknesses promoted the occurrence of instabilities. Conversely, moderate extrusion rates, appropriate die geometries, and low viscous components at the die wall consistently favored the stability of the combined flow. Of course, both encapsulation and interface instability phenomena could occur simultaneously. However, the scope of our investigations was limited by the narrow processing range of PWS products and by the lack of viscoelastic data for low-moisture starch melts. The latter observation is important because, in many cases, elastic properties of polymer melts are believed to be equally important to the mechanism of interfacial instabilities, as stated by Su and Khomami.[27] Finally, the interfacial strength of multilayer films could be improved by a controlled extent of instabilities at the interface by mechanical interlocking between respective layers.

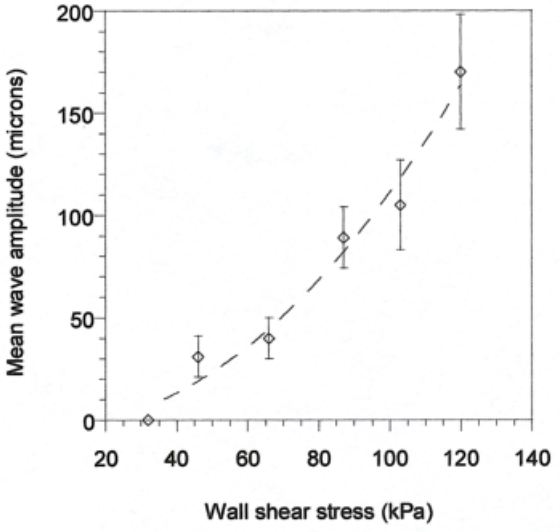

(a)

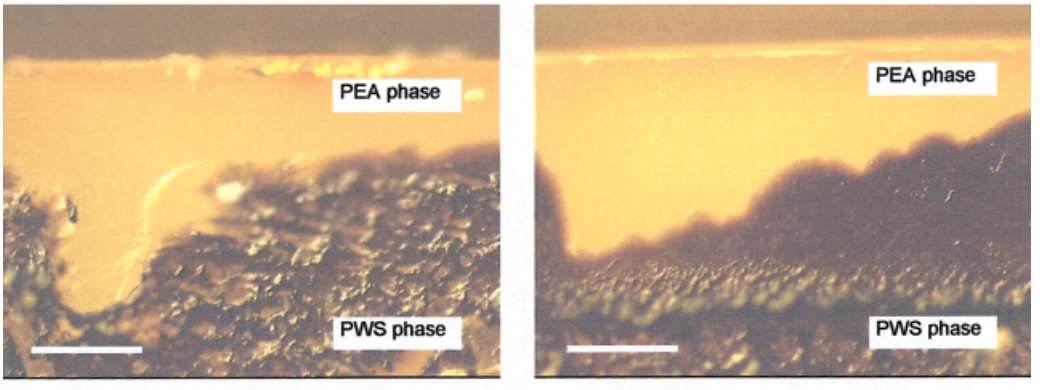

(b) (c)

Figure 12 (a) Mean wave amplitude as a function of shear stress and (b, c) illustration of the mechanical interlocking between layers for PEA/PWS2/PEA films. The white scale bar is 100 μm.

Future work in this area should take into account the elasticity effects of plasticized starch and that of the adjacent polymer on the flow instability mechanisms and should determine its importance compared to other factors. The effect of molecular structure and the density of polymers on interfacial instability may also be investigated. Finally, more attention should be focused on the exact location of incipient instabilities within the die.

This work was funded by Europol'Agro through a research program devoted to the study and development of new packaging materials based on renewable resources. The authors wish to thank Bayer for supplying the polyester materials.

References

1. Lörcks, J. J Polym Degrad Stab 1998, 59, 245.
2. Colonna, P.; Tayeb, J., Mercier, C. In Extrusion-Cooking; Mercier, C.; Linko, P.; Harper, J. M., Eds.; American Association of Cereal Chemists: St. Paul, MN, 1989; p 247.
3. Funke, U., Bergthaller, W.; Lindhauer, M. G. J Polym Degrad Stab 1998, 59, 293.
4. Avérous, L.; Frigant, C.; Moro, L. Starch/Stärke 2001, 53, 368.
5. Avérous, L.; Moro, L.; Dole, P. Polymer 2000, 41, 4157.
6. Martin, O.; Avérous, L. Polymer 2001, 42, 6209.
7. Avérous, L.; Fauconnier, N.; Moro, L.; Fringant, C. J Appl Polym Sci 2000, 76, 1117.
8. Avérous, L.; Fringant, C. Polym Eng Sci 2001, 41, 727.
9. Shogren, R. L.; Lawton, J. W. U.S. Pat. 5,756,194 (1998).
10. Schrenk, W. J.; Alfrey, T., Jr. In Polymer Blends; Paul, D. R.; Newman, S., Eds.; Academic Press: London, 1978; Vol 2.
11. Lee, B. L.; White, J. L. Trans Soc Rheo 1974, 18, 467.

12. Southern, J. H.; Ballman, R. L. J Appl Polym Sci 1973, 20, 175.
13. Khan, A. A.; Han, C. D. Trans Soc Rheol 1976, 20, 595.
14. White, J. L.; Ufford, R. C.; Dharod, K. R.; Price, R. L. J Appl Polym Sci 1972, 16, 1313.
15. Dooley, J.; Stout, B. Soc Plast Eng Annu Tech Conf 1991, 37, 62.
16. Dooley, J.; Hyun, K. S.; Hughes, K. Polym Eng Sci 1998, 38, 1060.
17. Yih, C. S. J Fluid Mech 1967, 27, 337.
18. Hickox, C. E. Phys Fluids 1971, 14, 251.
19. Schrenk, W. J.; Bradley, N. L.; Alfrey, T., Jr.; Maack, H. Polym Eng Sci 1978, 18, 620.
20. Han, C. D.; Shetty, R. Polym Eng Sci 1976, 16, 697.
21. Han, C. D.; Shetty, R. Polym Eng Sci 1978, 18, 180.
22. Karagiannis, A.; Mavridis, H.; Hrymak, A. N.; Vlachopoulos, J. Polym Eng Sci 1988, 28, 982.
23. Sornberger, G.; Vergnes, B.; Agassant, J. F. Polym Eng Sci 1986, 26, 451.
24. Gifford, W. A. Polym Eng Sci 1997, 37, 315.
25. Khomami, B. J Non-Newtorian Fluid Mech 1990, 36, 289.
26. Su, Y. Y.; Khomami, B. J Rheol 1992, 36, 357.
27. Su, Y. Y.; Khomami, B. Rheol Acta 1992, 31, 413.
28. Wilson, G. M.; Khomami, B. J Non-Newtonian Fluid Mech 1992, 45, 355.
29. Wilson, G. M.; Khomami, B. J Rheol 1993, 37, 315.
30. Tzoganakis, C.; Perdikoulias, J. Polym Eng Sci 2000, 40, 1056.
31. Wang, L.; Shogren, R. L.; Carriere, C. Polym Eng Sci 2000, 40, 499.
32. Martin, O.; Avérous, L.; Della Valle, G.; Couturier, Y. Cereal Chem, to appear.
33. Perdikoulias, J.; Richard, C.; Vlcek, J.; Vlachopoulos, J. ANTEC'91 1991, 2461.
34. Puissant, S.; Demay, Y.; Vergnes, B.; Agassant, J. F. Polym Eng Sci 1994, 34, 201.
35. Mavradis, H.; Schroff, R. Polym Eng Sci 1994, 34, 559.
36. Martin, O.; Schwach, E.; Avérous, L.; Couturier, Y. Starch/Stärke 2001, 37.
37. Ranjbaran, M. M.; Khomami, B. Polym Eng Sci 1996, 36, 1875.